

# Correlation Between Cloud Adjustments and Cloud Feedbacks Responsible for Larger Range of Climate Sensitivities in CMIP6

Nicholas J. Lutsko<sup>1</sup>, Matthew T. Luongo<sup>1</sup>, Casey J. Wall<sup>1</sup>, Timothy A. Myers<sup>2,3</sup>

<sup>1</sup>Scripps Institution of Oceanography, University of California at San Diego, La Jolla, California, USA.

<sup>2</sup>Cooperative Institute for Research in Environmental Sciences (CIRES), University of Colorado, Boulder, Colorado, USA

<sup>3</sup>Physical Science Laboratory, National Oceanic and Atmospheric Administration, Boulder, Colorado, USA

## Key Points:

- The relationship between feedback and forcing is sensitive to the definition of the forcing, especially in CMIP6
- Cloud adjustments are anti-correlated with cloud feedbacks in CMIP5 and positively correlated in CMIP6
- It is unclear what caused this change, though models derived from a small number of modeling centers drive the trend

## Abstract

While the higher mean Equilibrium Climate Sensitivity (ECS) in CMIP6 has been attributed to more positive cloud feedbacks, it is unclear what causes the greater range of ECS values across CMIP6 models compared to CMIP5. Here we investigate the relationship between radiative forcing and cloud feedbacks across the two model generations to explain the very high ECS values in some CMIP6 models. The relationship is sensitive to the definition of the forcing, particularly in CMIP6, but fixed-SST simulations suggest the shortwave cloud feedback ( $\lambda_{SW,cl}$ ) is anti-correlated with the forcing in CMIP5 and weakly positively correlated with the forcing in CMIP6. These relationships reflect the cloud adjustment to the forcing, which is anti-correlated with  $\lambda_{SW,cl}$  in CMIP5 and positively correlated in CMIP6. Although we are unable to identify a systematic change across the model generations, we do show that modifications to the land components of climate models are not responsible for the change in the relationship between cloud adjustments and cloud feedbacks, and that cloud adjustments are generally driven by low and, especially mid-level clouds. Moreover, models derived from the MOHC and NCAR modeling centers seem to be responsible for much of the trend between CMIP5 and CMIP6. Our analysis is severely limited by the available simulations, highlighting the need for targeted simulations to probe the sources of intermodel differences in cloud adjustments.

## 1 Introduction

The models participating in the Sixth Climate Model Intercomparison Project (CMIP6) have a much wider range of Equilibrium Climate Sensitivities (ECSs) than the models participating in the Fifth Climate Model Intercomparison Project (CMIP5): in CMIP6 the lowest ECS is 1.83K (INM-CM4-8) and the highest ECS is 5.64K (CanESM5), while in CMIP5 the corresponding values are 2.08K (INM-CM-4) and 4.65K (MIROC-ESM) [Zelinka *et al.*, 2020]. The high end of the CMIP6 models' ECS in particular has been the subject of much concern, as the fact that several CMIP6 models have ECS values  $\geq 5K$  raises the possibility of a very high real-world ECS. While the move away from raw model weighting and towards combining multiple lines of evidence to assess ECS have led both the recent Sherwood *et al.* [2020] assessment and the IPCC's AR6 report [Forster *et al.*, 2021] to place the upper bound of ECS below 5K, it is still important to understand what causes these high sensitivities so that the realism of the models can be evaluated.

45 The high sensitivities also raise the possibility that models contain undiagnosed physical  
 46 processes or feedbacks not included in the evaluation of *Sherwood et al.* [2020].

47 ECS is determined by the radiative forcing due to a doubling of CO<sub>2</sub>,  $F$ , divided by  
 48 the climate feedback parameter, or radiative restoring co-efficient,  $\lambda$ :

$$ECS = \frac{F}{\lambda}. \quad (1)$$

49  $F$  is typically taken to include both the instantaneous radiative forcing (IRF) from in-  
 50 creased CO<sub>2</sub> concentrations and the “rapid adjustments” to the forcing which appear in  
 51 the first few days or weeks after CO<sub>2</sub> increase [*Hansen et al.*, 2005; *Gregory and Webb*,  
 52 2008; *Sherwood et al.*, 2015]. These rapid adjustments come from increases in land tem-  
 53 peratures, decreases in stratospheric temperatures and changes in atmospheric properties  
 54 that are directly forced by CO<sub>2</sub> and not mediated by surface temperature changes. The to-  
 55 tal feedback  $\lambda$  includes both clear-sky and cloud feedbacks, with the latter typically taken  
 56 to be the largest source of uncertainty in ECS [e.g., *Soden et al.*, 2008; *Vial et al.*, 2013;  
 57 *Forster et al.*, 2013; *Zelinka et al.*, 2020; *Sherwood et al.*, 2020].

58 In addition to a larger range of ECS values, the CMIP6 models also have a higher  
 59 ensemble-mean ECS than the CMIP5 models. The latter was attributed by *Zelinka et al.*  
 60 [2020] to a more positive ensemble-mean cloud feedback, specifically an increase in the  
 61 shortwave low cloud feedback. This is driven by a more positive extratropical low cloud  
 62 amount feedback and more positive SW low cloud scattering feedback in all regions [see  
 63 also *Lutsko et al.*, 2021]. However, while cloud feedbacks can explain the higher mean  
 64 ECS, the range of total feedbacks is similar in both sets of models, as is the range of net  
 65 (longwave plus shortwave) cloud feedbacks (see Figure 1c of *Zelinka et al.* [2020]); long-  
 66 wave cloud feedbacks compensate to some extent for shortwave cloud feedbacks. Thus  
 67 feedbacks alone cannot explain the very high ECS CMIP6 models. Instead, as *Zelinka*  
 68 *et al.* note, the highest ECS models in CMIP6 combine moderate radiative forcings with  
 69 weak (negative) climate feedback parameters in a way that wasn’t seen in CMIP5: the  
 70 most sensitive models in CMIP5 have both weak climate feedback parameters and weak  
 71 forcings, which limits the maximum ECS values.

72 In this study, we investigate the relationships between forcings and cloud feedbacks  
 73 in the two generations of models, seeking to explain why the combination of moderate  
 74 forcing and small climate feedback parameter is present in some CMIP6 models but in  
 75 none of the CMIP5 models. We draw on a number of previous studies that have estimated

76 radiative forcings and feedbacks in CMIP5 and CMIP6 models (see next section) and  
 77 compare different ways of estimating the radiative forcing, which turns out to be essential  
 78 for clarifying the relationships between forcings and feedbacks across model generations.  
 79 Our analysis is severely limited by the small number of fixed Sea Surface Temperature  
 80 (SST) simulations in both ensembles, particularly CMIP5. Fixed-SST simulations are re-  
 81 quired to accurately estimate radiative forcing and to investigate what causes differences in  
 82 radiative forcing between models. Nevertheless, using the available data we do find sug-  
 83 gestive evidence that, rather than systematic differences between model generations, the  
 84 changes are primarily driven by models derived from two modeling centers, which com-  
 85 bine strong, positive cloud feedbacks and large, positive cloud adjustments to forcing.

## 86 2 Data Sources

87 The following data sources are used in the analysis:

- 88 • Regression-based forcing estimates, using years 1-140 of abrupt-4XCO<sub>2</sub> simula-  
 89 tions, for 24 CMIP5 models and 31 CMIP6 models from *Zelinka et al.* [2020].
- 90 • Shortwave cloud feedbacks ( $\lambda_{SW,cl}$ ) for 24 CMIP5 models and 31 CMIP6 models  
 91 from *Zelinka et al.* [2020].
- 92 • Regression-based forcing estimates, using years 1-20 of abrupt-4XCO<sub>2</sub> simulations,  
 93 for 24 CMIP5 models and 29 CMIP6 models from *Dong et al.* [2020].
- 94 • Fixed-SST forcing estimates for 13 CMIP5 models from *Kamae and Watanabe*  
 95 [2012].
- 96 • Fixed-SST forcing estimates for 17 CMIP6 models from *Smith et al.* [2020].
- 97 • Estimates of the Cloud Radiative Effect (CRE) response to CO<sub>2</sub> forcing for 13  
 98 CMIP5 models from *Kamae and Watanabe* [2012]. Note that the CRE response  
 99 is not equivalent to the cloud adjustment to the forcing as it does not account for  
 100 cloud masking [*Soden et al.*, 2004], but it is well correlated with estimates of the  
 101 true cloud adjustment (see next bullet).
- 102 • Estimates of the cloud adjustment to the forcing for six CMIP5 models (CanESM2,  
 103 CCSM4, HadGEM2-A, IPSL-CM5A-LR, MIROC5 and MRI-CGCM3) are calcu-  
 104 lated following the procedure in *Zelinka et al.* [2013]. These are the models which

105 ran fixed-SST simulations with the ISCCP simulator<sup>1</sup> and thus provided the neces-  
 106 sary data to estimate the true cloud adjustment.

- 107 • Estimates of the cloud adjustments to the forcing for 16 CMIP6 models from *Smith*  
 108 *et al.* [2020], including 10 CMIP6 models which ran fixed-SST simulations with  
 109 the ISCCP simulator. Note that we have calculated the cloud adjustment for the  
 110 MIROC6 model using the *Zelinka et al.* [2013] method, which was not included in  
 111 the analysis of *Smith et al.* [2020].
- 112 • Cloud adjustments in aquaplanet simulations with seven CMIP6 models, calculated  
 113 following the procedure in *Zelinka et al.* [2013].
- 114 • Meteorological cloud radiative kernels from *Myers et al.* [2021] based on the Cloud  
 115 Controlling Factor (CCF) analysis developed by *Scott et al.* [2020] for five CMIP5  
 116 models and seven CMIP6 models. Note that we have calculated a new CCF kernel  
 117 for the CESM2 model as part of this analysis. The required meteorological data for  
 118 the CCF analysis were also downloaded for each model (see Supplementary Text  
 119 for more information).

120 See Tables 1 and 2 for complete lists of models and data used in this study. All val-  
 121 ues are linearly scaled for a doubling of CO<sub>2</sub>, e.g., if 4XCO<sub>2</sub> values are reported, we have  
 122 divided them by 2.

### 145 3 Different Forcing Definitions

146 We begin by investigating the relationships between different forcing definitions.  
 147 The simplest way of estimating radiative forcing is through so-called “Gregory” regres-  
 148 sions [*Gregory et al.*, 2004], in which the anomalous surface temperature ( $T$ ) from abrupt-  
 149 4XCO<sub>2</sub> simulations is regressed onto the anomalous net top-of-atmosphere (TOA) radia-  
 150 tive flux ( $R$ ). The forcing is defined as the y-intercept of the regression. *Zelinka et al.*  
 151 [2020] diagnosed the forcings in CMIP5 and CMIP6 by regressing  $R$  onto  $T$  for years  
 152 1-140 of the abrupt-4XCO<sub>2</sub> simulations in the two sets of simulations. These forcing esti-  
 153 mates ( $F_{1-140}$ ) are problematic, however, as the radiative feedback  $\lambda$  (the slope of  $R$  over  
 154  $T$ ) changes over time due to the so-called “pattern effect” in which evolving patterns of

---

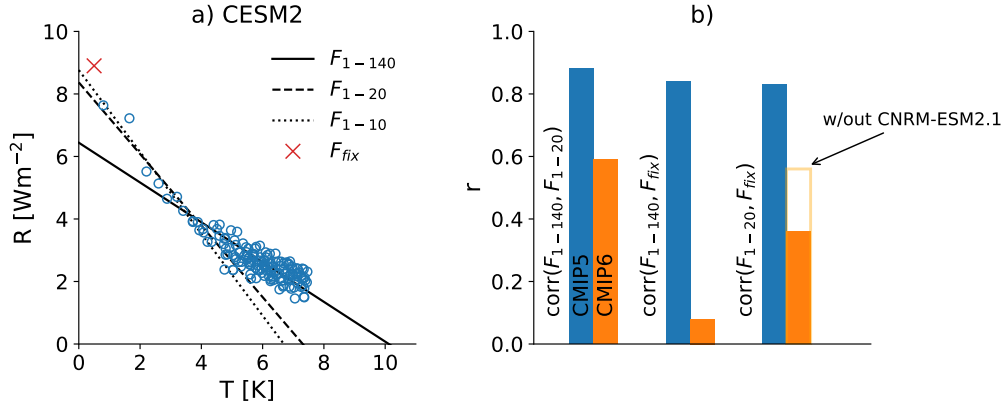
<sup>1</sup> The International Satellite Cloud Climatology Project (ISCCP) simulator translates modeled cloud fields into a distri-  
 bution of cloud fractions as a joint function of seven cloud-top pressure ranges and seven cloud optical depth ranges, in an  
 analogous manner to the observational ISCCP cloud product [*Klein and Jakob*, 1999; *Webb et al.*, 2001]

123 **Table 1.** CMIP5 models used in this study. Where available, regression-based forcing estimates, using  
 124 years 1-140 of abrupt-4XCO<sub>2</sub> simulations ( $F_{1-140}$ ), are taken from *Zelinka et al. [2020]*, regression-based  
 125 forcing estimates, using years 1-20 of abrupt-4XCO<sub>2</sub> simulations ( $F_{1-20}$ ), are taken from *Dong et al. [2020]*,  
 126 fixed-SST forcing estimates ( $F_{fix}$ ) are taken from *Kamae and Watanabe [2012]*, short-wave cloud feedbacks  
 127  $\lambda_{SW,cl}$  are taken from *Zelinka et al. [2020]*, estimates of the Cloud Radiative Effect (CRE) response to CO<sub>2</sub>  
 128 forcing are taken from *Kamae and Watanabe [2012]* and estimates of the cloud adjustment to the forcing are  
 129 calculated following the procedure in *Zelinka et al. [2013]*.

Model	$F_{1-140}$ [Wm <sup>-2</sup> ]	$F_{1-20}$ [Wm <sup>-2</sup> ]	$F_{fix}$ [Wm <sup>-2</sup> ]	$\lambda_{SW,cl}$ [Wm <sup>-2</sup> /K]	$\Delta CRE$ [Wm <sup>-2</sup> ]	Cloud adjustment [Wm <sup>-2</sup> ]
ACCESS1.0	2.94	3.56	–	0.07	–	–
ACCESS1.3	2.88	3.42	–	0.48	–	–
BCC-CSM1.1	3.24	3.78	–	-0.15	–	–
BCC-CSM1.1-M	3.43	3.85	–	-0.02	–	–
CanESM2	3.81	4.18	3.67	-0.29	-0.02	0.63
CCSM4	3.48	4.08	4.42	-0.09	0.19	0.96
CNRM-CM5	3.69	3.58	3.93	-0.21	-0.01	–
CSIRO-Mk3.6.0	2.60	3.55	3.10	0.55	-0.73	–
GFDL-CM3	3.01	3.70	–	0.6	–	–
GFDL-ESM2G	2.99	3.50	–	-0.4	–	–
GFDL-ESM2M	3.35	3.58	–	-0.49	–	–
GISS-E2-H	3.82	4.11	–	-0.72	–	–
GISS-E2-R	3.73	4.64	–	-0.8	–	–
HadGEM2-ES	2.91	3.33	3.50	0.29	-0.06	0.37
INM-CM4	2.97	3.06	3.12	-0.02	-0.57	–
IPSL-CM5A-LR	3.10	3.36	3.25	0.61	-0.28	-0.05
IPSL-CM5A-MR	3.31	3.50	–	0.62	–	–
IPSL-CM5B-LR	2.65	3.03	–	0.35	–	–
MIROC5	4.16	4.38	3.97	-0.38	-0.21	0.61
MPI-ESM-LR	4.10	4.58	4.31	-0.16	0.10	–
MPI-ESM-MR	4.11	4.68	4.30	-0.07	0.12	–
MPI-ESM-P	4.27	4.91	4.30	-0.21	0.11	–
MRI-CGCM3	3.20	3.60	3.60	0.25	-0.42	0.06
NorESM1-M	3.16	3.77	3.48	-0.02	0.04	–

130 **Table 2.** CMIP6 models used in this study. Where available, regression-based forcing estimates, using  
 131 years 1-140 of abrupt-4XCO2 simulations ( $F_{1-140}$ ), are taken from *Zelinka et al.* [2020], regression-based  
 132 forcing estimates, using years 1-20 of abrupt-4XCO2 simulations ( $F_{1-20}$ ), are taken from *Dong et al.* [2020],  
 133 fixed-SST forcing estimates ( $F_{fix}$ ) are taken from *Smith et al.* [2020], short-wave cloud feedbacks  $\lambda_{SW,cl}$  are  
 134 taken from *Zelinka et al.* [2020], estimates of the cloud adjustment to the forcing are taken from *Smith et al.*  
 135 [2020] and estimates of the cloud adjustment in aquaplanet simulations are calculated following the procedure  
 136 in *Zelinka et al.* [2013]

Model	$F_{1-140}$ [ $\text{Wm}^{-2}$ ]	$F_{1-20}$ [ $\text{Wm}^{-2}$ ]	$F_{fix}$ [ $\text{Wm}^{-2}$ ]	$\lambda_{SW,cl}$ [ $\text{Wm}^{-2}/\text{K}$ ]	Cloud adjustment [ $\text{Wm}^{-2}$ ]	Aquaplanet cloud adjustment [ $\text{Wm}^{-2}$ ]
ACCESS-CM2	3.43	4.12	3.97	0.96	0.70	–
ACCESS-ESM1-5	2.83	3.50	–	0.43	–	–
BCC-CSM2-MR	3.11	3.59	–	0.16	–	–
BCC-ESM1	3.01	3.47	–	0.02	–	–
CAMS-CSM1.0	4.17	4.33	–	-0.72	–	–
CESM2-WACCM	3.30	4.05	–	1.05	–	–
CESM2	3.27	4.18	4.45	0.79	1.07	1.62
CNRM-CM6.1	3.64	3.95	4.00	-0.02	0.22	0.20
CNRM-ESM2.1	2.97	2.79	3.96	0.03	0.12	–
CanESM5	3.68	3.75	3.80	-0.02	0.47	–
E3SM-1.0	3.33	3.68	–	0.75	–	–
EC-Earth3-Veg	3.22	4.00	–	0.02	–	–
EC-Earth3	3.37	4.00	4.05	0.05	–	–
GFDL-CM4	3.19	4.23	4.22	0.03	0.56	0.52
GFDL-ESM4	3.77	3.69	3.87	-0.15	0.62	–
GISS-E2.1-G	3.95	4.00	3.67	-0.63	0.12	–
GISS-E2.1-H	3.53	3.72	–	-0.53	–	–
HadGEM3-GC31-LL	3.49	3.87	4.05	0.98	0.74	0.58
INM-CM4.8	2.70	3.13	–	-0.19	–	–
INM-CM5.0	2.92	3.14	–	-0.11	–	–
IPSL-CM6A-LR	3.58	3.90	4.00	0.14	0.47	0.16
MIROC-ES2L	4.11	3.98	–	-0.35	–	–
MIROC6	2.65	3.65	3.66	-0.13	0.35	0.47
MPI-ESM1.2-LR	4.22	–	4.17	-0.68	0.70	–
MPI-ESM1.2-HR	3.65	4.18	–	-0.41	–	–
MRI-ESM2.0	3.43	3.99	3.83	0.12	0.29	0.72
NESM3	3.73	4.91	–	-0.15	–	–
NorESM2-LM	3.43	4.61	4.07	0.21	0.72	–
NorESM2-MM	3.73	–	4.19	0.30	0.78	–
SAM0-UNICON	3.89	4.18	–	0.89	–	–
UKESM1.0-LL	3.61	3.82	3.97	0.93	0.80	–



137 **Figure 1.** a) “Gregory” plot of  $R$  against  $T$  for a representative CMIP6 model (CESM2). The blue mark-  
 138 ers show annual-mean values, the solid line shows a regression of  $R$  against  $T$  using all 140 years of data,  
 139 the dashed line shows a regression using only years 1-20 and the dotted line shows a regression using years  
 140 1-20. The regression-based forcings are taken to be the y-intercepts of these lines. The red cross shows the  
 141 fixed-SST forcing  $F_{fix}$ . b) Pearson correlation coefficients ( $r$ ) between the different forcing estimates for the  
 142 CMIP5 data (blue) and the CMIP6 (orange). The empty orange bar in the third column shows  $r$  when CNRM-  
 143 ESM2.1 (whose abrupt4XCO2 simulation was set up incorrectly, leading to an anomalously small  $F_{1-20}$ ) is  
 144 excluded from the correlation.

155 warming cause  $\lambda$  to change over time [Winton *et al.*, 2010; Armour *et al.*, 2013; Geoffroy  
 156 *et al.*, 2013; Andrews *et al.*, 2015; Xie, 2020]. Plots of  $R$  against  $T$  typically feature in-  
 157 flection points about 20 years after the increase in  $\text{CO}_2$  and so, since  $\lambda$  decreases over  
 158 time, regressing over all 140 years will typically lead to an underestimate of  $F$  (see Figure  
 159 1a). For the same reason,  $F_{1-140}$  will tend to be correlated across models with  $\lambda$ : a model  
 160 with a smaller (less negative)  $\lambda$  will have a smaller  $F_{1-140}$ . The correlation between  $\lambda$  and  
 161  $F_{1-140}$  further implies a correlation between  $F_{1-140}$  and  $\lambda_{SW,CL}$ , since  $\lambda_{SW,CL}$  is the main  
 162 source of uncertainty in  $\lambda$ . This partly explains the statistically significant correlations be-  
 163 tween  $F$  and  $\lambda_{SW,CL}$  found in previous studies [see below and e.g., Caldwell *et al.*, 2016].

164 To obtain forcing estimates that do not depend so directly on  $\lambda$ , we consider two  
 165 other ways of estimating  $F$ . First,  $F$  can be diagnosed by regressing  $T$  onto  $R$  over the  
 166 first 20 years of the abrupt 4XCO2 simulations ( $F_{1-20}$ ), as used e.g., by Dong *et al.* [2020].  
 167 These estimates are more independent of the feedback but, as noted by Forster *et al.* [2016],  
 168 regression-based estimates of  $F$  are sensitive to the number of years included in the re-  
 169 gressions:  $F_{1-10}$  will differ slightly from  $F_{1-20}$  (see Figure 1a). Second, we take estimates

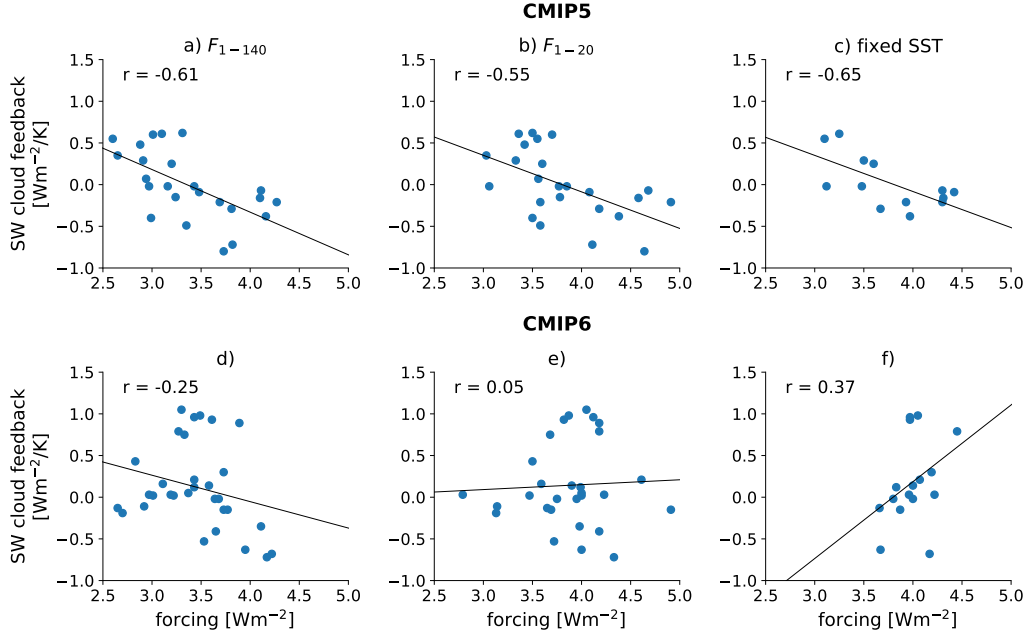
170 of  $F$  from simulations in which atmospheric  $\text{CO}_2$  concentrations are quadrupled but SSTs  
 171 are kept fixed ( $F_{fix}$ ). Taking the difference between these and control simulations gives  
 172 forcing estimates that include both the IRF and the rapid adjustments.  $F_{fix}$  does not de-  
 173 pend explicitly on  $\lambda$  and is not sensitive to the number of years included in the analysis  
 174 provided that the forcing is estimated over a long enough time period for internal variabil-  
 175 ity to be small.

176 In CMIP5 these three sets of forcing estimates are well correlated (blue bars in Fig-  
 177 ure 1b), though  $F_{1-140}$  is almost always smaller than  $F_{1-20}$  and  $F_{fix}$  (Supplemental Figure  
 178 S1). By contrast, in CMIP6 the correlation between  $F_{1-140}$  and  $F_{1-20}$  is much lower and  
 179 the correlation between  $F_{1-140}$  and  $F_{fix}$  is negligible (orange bars in Figure 1b).  $F_{1-20}$  and  
 180  $F_{fix}$  are weakly correlated in CMIP6 ( $r = 0.36$ ), though note that the 4XCO2 simulations  
 181 with CNRM-ESM2.1 were not set up correctly [Smith *et al.*, 2020], leading to an anoma-  
 182 lously small value of  $F_{1-20}$  (see panel e of Supplemental Figure S1). Without this outlier  
 183 model, the correlation between  $F_{1-20}$  and  $F_{fix}$  is substantially higher ( $r = 0.56$ ). Hereafter,  
 184 we take  $F_{1-20}$  and  $F_{fix}$  to be more representative of models' true radiative forcings than  
 185 the  $F_{1-140}$  estimates used by Zelinka *et al.* [2020].

#### 186 **4 Relationships Between Forcings and Cloud Feedbacks**

187 We now examine the relationship between  $F$  and  $\lambda_{SW,CL}$  in the two sets of mod-  
 188 els. Figure 2a-c shows that whatever forcing definition is used,  $F$  and  $\lambda_{SW,CL}$  are anti-  
 189 correlated in the CMIP5 models [see also Caldwell *et al.*, 2016]. That is, even  $F_{1-20}$  and  
 190  $F_{fix}$ , which are not directly related to the long-term value of  $\lambda$ , have an inverse relation-  
 191 ship with  $\lambda_{SW,CL}$  in the CMIP5 models.

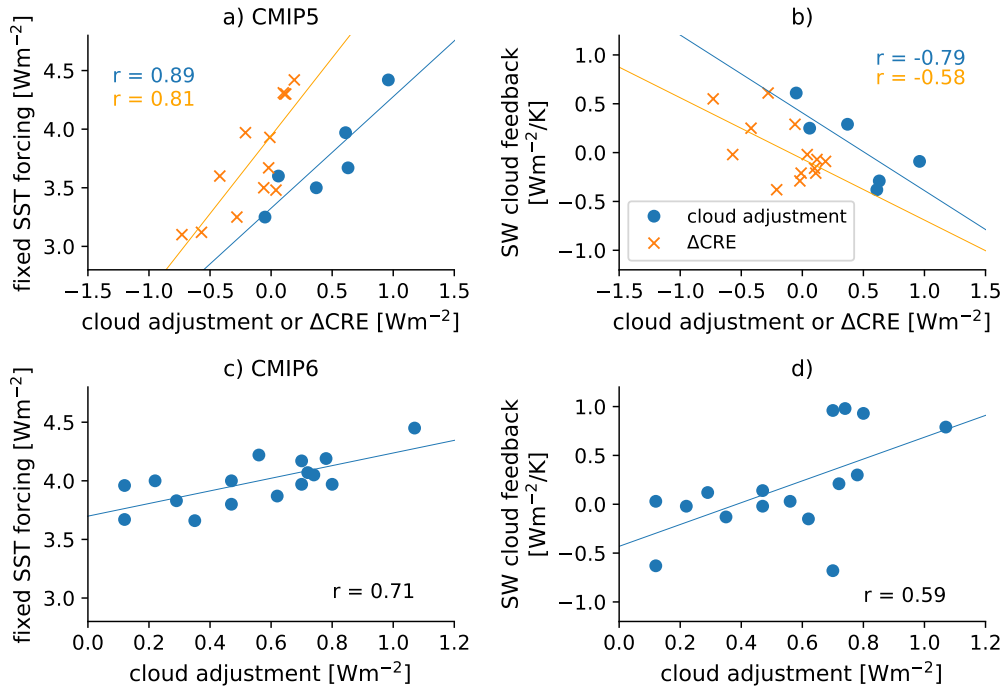
197 By contrast, there is no relationship between  $F_{1-20}$  and  $\lambda_{SW,CL}$  in the CMIP6 mod-  
 198 els ( $r = 0.05$ , Figure 2e), while  $F_{fix}$  and  $\lambda_{SW,CL}$  are weakly positively correlated ( $r =$   
 199  $0.37$ , Figure 2f).  $F_{1-140}$  and  $\lambda_{SW,CL}$  are anti-correlated in CMIP6, as expected from the  
 200 discussion in the previous section (Figure 2d), though the relationship is much weaker  
 201 than in CMIP5 ( $r = -0.25$  versus  $r = -0.61$ ). Given the discussion above and in Forster  
 202 [2016], we take the fixed SST estimates to be the most reliable forcing estimates, such that  
 203 the forcing and the SW cloud feedback are anti-correlated in CMIP5 and weakly positively  
 204 correlated in CMIP6.



192 **Figure 2.** Relationships between the SW cloud feedback  $\lambda_{SW,cl}$  and different forcing definitions in CMIP5  
 193 and CMIP6. a)  $\lambda_{SW,cl}$  versus  $F_{1-140}$  in CMIP5, b)  $\lambda_{SW,cl}$  versus  $F_{1-20}$  in CMIP5, c)  $\lambda_{SW,cl}$  versus  $F_{fix}$   
 194 in CMIP5, d)  $\lambda_{SW,cl}$  versus  $F_{1-140}$  in CMIP6, e)  $\lambda_{SW,cl}$  versus  $F_{1-20}$  in CMIP6, f)  $\lambda_{SW,cl}$  versus  $F_{fix}$  in  
 195 CMIP6. In all panels the Pearson correlation coefficient  $r$  is shown in the upper left and the lines show linear  
 196 least-squares regressions.

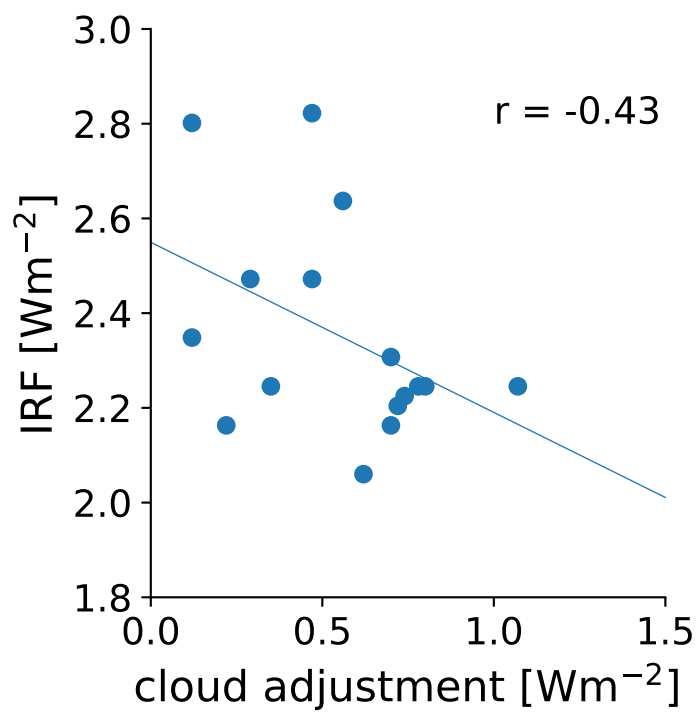
## 212 5 Cloud Adjustments and Cloud Feedbacks

213 The most likely candidate to explain the relationships between forcings and cloud  
 214 feedbacks is the cloud adjustment to the forcing. Unfortunately, only six modeling centers  
 215 ran fixed SST simulations with ISCCP simulators in CMIP5, which are needed to estimate  
 216 the cloud adjustments using the *Zelinka et al. [2013]* methodology. For this reason, we  
 217 have also used the change in Cloud Radiative Effect ( $\Delta CRE$ ), as diagnosed for 13 CMIP5  
 218 models by *Kamae and Watanabe [2012]*, to investigate the relationships between cloud  
 219 adjustments, total forcings and cloud feedbacks. 10 CMIP6 models ran fixed SST simula-  
 220 tions with the ISCCP simulator, and *Smith et al. [2020]* estimated the forcing for six addi-  
 221 tional models using other methods (the approximate partial radiative perturbation method  
 222 and the offline monthly-mean partial radiative perturbation method).

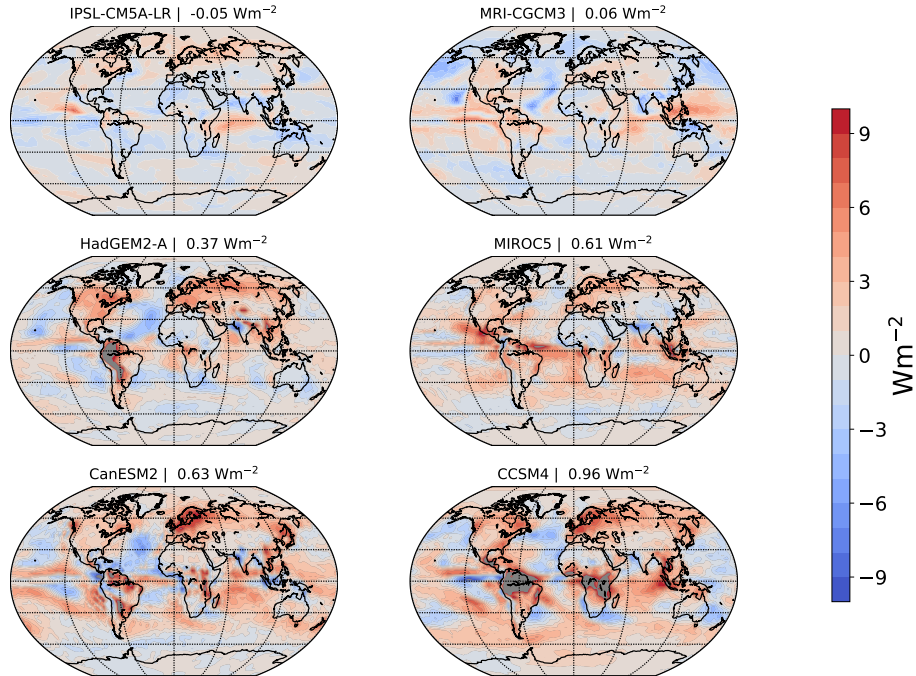


205 **Figure 3.** Relationships between cloud adjustments, the fixed-SST forcings and the SW cloud feedbacks. a)  
 206 Fixed SST forcing  $F_{fix}$  versus the cloud adjustment in CMIP5 (blue circles), and versus the change in CRE  
 207 in fixed-SST CMIP5 simulations (orange crosses). b) SW cloud feedback  $\lambda_{SW,cl}$  versus the cloud adjustment  
 208 in CMIP5 (blue circles), and versus the change in CRE in fixed-SST CMIP5 simulations (orange crosses).  
 209 c) Fixed SST forcing  $F_{fix}$  versus the cloud adjustment in CMIP6. d) SW cloud feedback  $\lambda_{SW,cl}$  versus the  
 210 cloud adjustment in CMIP6. The Pearson correlation coefficients are indicated on each panel and the lines  
 211 show linear least-squares regressions.

225 The cloud adjustment is positively correlated with the forcing and anti-correlated  
 226 with the SW cloud feedback in CMIP5, consistent with the results of the previous section  
 227 (Figure 3a-b). IPSL-CM5A-LR, which has the largest SW cloud feedback, has a small,  
 228 negative cloud adjustment, while CCSM4 has the largest cloud adjustment and a nega-  
 229 tive SW cloud feedback (see Table 1). This anti-correlation was also noted for CMIP5 by  
 230 *Chung and Soden* [2015], though they examined the CRE responses for both the adjust-  
 231 ments and the feedbacks in CMIP5, not the “true” cloud adjustments and cloud feedbacks.  
 232 In CMIP6 the cloud adjustment is positively correlated with both the fixed-SST forcing  
 233 estimates (Figure 3c) and the SW cloud feedbacks (Figure 3d). Interestingly, in CMIP6



223 **Figure 4.** Cloud adjustment versus IRF in the 16 CMIP6 models analyzed by *Smith et al.* [2020]. The  
224 Pearson correlation coefficient is given in the top right and the line shows the linear least-square regression.

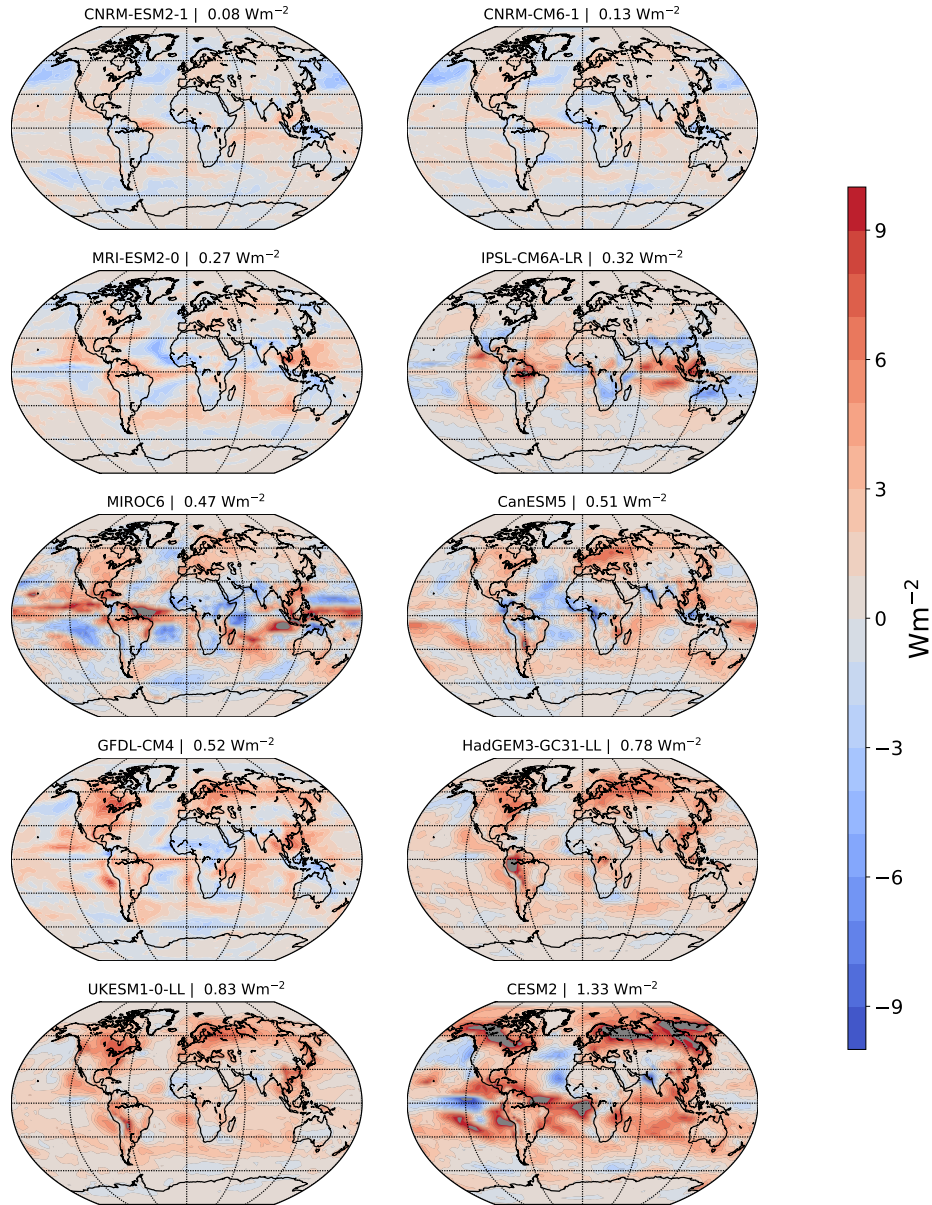


243 **Figure 5.** Spatial maps of the net cloud adjustments in the six CMIP5 models which ran fixed-SST simu-  
 244 lations with the ISCCP simulator. The global-mean net cloud adjustment is given above each panel, and the  
 245 models are ordered by the size of their adjustment. Values outside the colorbar range are shaded in gray.

234 the cloud adjustment is anti-correlated with the IRF ( $r = -0.43$ , Figure 4). We have not  
 235 investigated this relationship further, and note that *Andrews et al.* [2019] mentioned the  
 236 possibility of such an anti-correlation in their investigation of the causes of higher sensi-  
 237 tivity in the HadGEM3-GC3.1-LL climate model. Anti-correlation between IRF and cloud  
 238 adjustments may explain why the relationships between the SW cloud feedback and the  
 239 total forcing metrics are weak in CMIP6, even though there is a more robust relationship  
 240 between  $\lambda_{SW,cl}$  and the cloud adjustments: since the total forcing is largely set by the sum  
 241 of the IRF and the cloud adjustment, anti-correlation between these may reduce the corre-  
 242 lation between the total forcing and the SW cloud feedback.

## 252 6 What Changed Between CMIP5 and CMIP6?

253 The relatively small number of fixed-SST simulations, especially in the CMIP5  
 254 archive, makes it difficult to uncover systematic differences between the two generations  
 255 of models. Moreover, cloud adjustments remain poorly understood compared to cloud  
 256 feedbacks, though it is known that they are driven by land-sea circulations and changes



246 **Figure 6.** Spatial maps of the net cloud adjustments in the ten CMIP6 models which ran fixed-SST simu-  
 247 lations with the ISCCP simulator. The global-mean net cloud adjustment is given above each panel, and the  
 248 models are ordered by the size of their adjustment. Values outside the colorbar range are shaded in gray. Note  
 249 that in some cases the global-mean cloud adjustments differ from the values in Table 2, which are the average  
 250 of the three methods used by *Smith et al.* [2020] to estimate cloud adjustments, whereas the values in this  
 251 figure only come from the *Zelinka et al.* [2013] method.

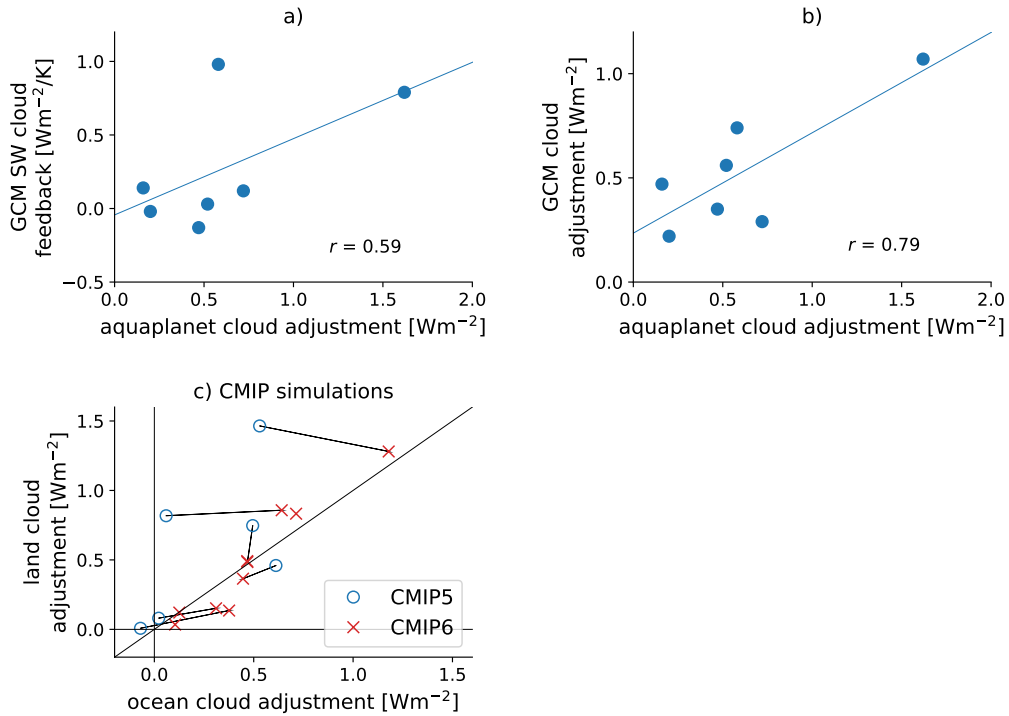
257 in atmospheric stability, among other things. There is also a diverse range of cloud adjust-  
 258 ment patterns across the models, and comparing the cloud adjustments in the six modeling  
 259 centers which provided fixed-SST simulations in both CMIP5 and CMIP6 (CCCMA, IPSL  
 260 NCAR, MIROC, MOHC, MRI) shows that the patterns of cloud adjustments are more  
 261 similar for models from the same modeling center than for models from the same genera-  
 262 tion (compare relevant panels in Figures 5 and 6).

263 Changes in cloud adjustments are also not obviously connected to changes in cloud  
 264 feedbacks:  $\lambda_{SW,cl}$  increased substantially in the two NCAR models (by  $+0.88\text{Wm}^{-2}/\text{K}$ )  
 265 and in the two MOHC models (by  $+0.69\text{Wm}^{-2}/\text{K}$ ), increased to a lesser extent in the  
 266 MIROC and CCCma models (by  $+0.25\text{Wm}^{-2}/\text{K}$  and  $+0.07\text{Wm}^{-2}/\text{K}$ , respectively) and  
 267 decreased in the MRI and IPSL models (by  $-0.13\text{Wm}^{-2}/\text{K}$  and  $-0.47\text{Wm}^{-2}/\text{K}$ , respec-  
 268 tively), while the largest increase in cloud adjustment is seen between the two IPSL mod-  
 269 els ( $+0.52\text{Wm}^{-2}$ ), then between the two MOHC models ( $+0.37\text{Wm}^{-2}$ ), between the MRI  
 270 models ( $+0.23\text{Wm}^{-2}$ ) and the NCAR models ( $+0.11\text{Wm}^{-2}$ ). The net cloud adjustment  
 271 decreased by  $-0.16\text{Wm}^{-2}$  between the CCCMa models and by  $-0.25\text{Wm}^{-2}$  between the  
 272 MIROC models (Figures 5 and 6). Hence changes in cloud adjustments cannot be pre-  
 273 dicted by changes in cloud feedbacks.

280 Nevertheless, we have worked with the available data to explore potential explana-  
 281 tions for the changes in behavior between the model generations. The first possibility we  
 282 investigated is that modifications to the land components of the models are responsible  
 283 for the changes between generations. We have also decomposed the net cloud adjustments  
 284 into contributions from different cloud types and used a cloud controlling factor analysis  
 285 to probe the causes of changes in low clouds. While neither analysis has shown conclu-  
 286 sively what changed between the model generations, these calculations have allowed us  
 287 to rule out certain possibilities and to identify key features of the changes between model  
 288 generations.

## 289 **6.1 Changes in land models**

290 Cloud adjustments are partly the result of circulations which arise due to differen-  
 291 tial warming of land surfaces and the ocean [assuming SSTs are kept fixed *Andrews et al.*,  
 292 2012; *Zelinka et al.*, 2013]. Between CMIP5 and CMIP6, the land components of many



274 **Figure 7.** a) Cloud adjustments in the aquaplanet CMIP6 simulations versus the SW cloud feedback. The  
 275 blue line shows a linear least-squares regression. b) Cloud adjustments in the aquaplanet CMIP6 simulations  
 276 versus the true cloud adjustments calculated from the fixed SST simulations. The blue line shows a linear  
 277 least-squares regression. c) Land and ocean contributions to the cloud adjustments in the comprehensive sim-  
 278 ulations. CMIP5 models are denoted by the open blue circles and CMIP6 models by the red crosses. The  
 279 diagonal black line shows the 1:1 line.

293 models were upgraded, which could drive changes in cloud adjustments between the gen-  
 294 erations.

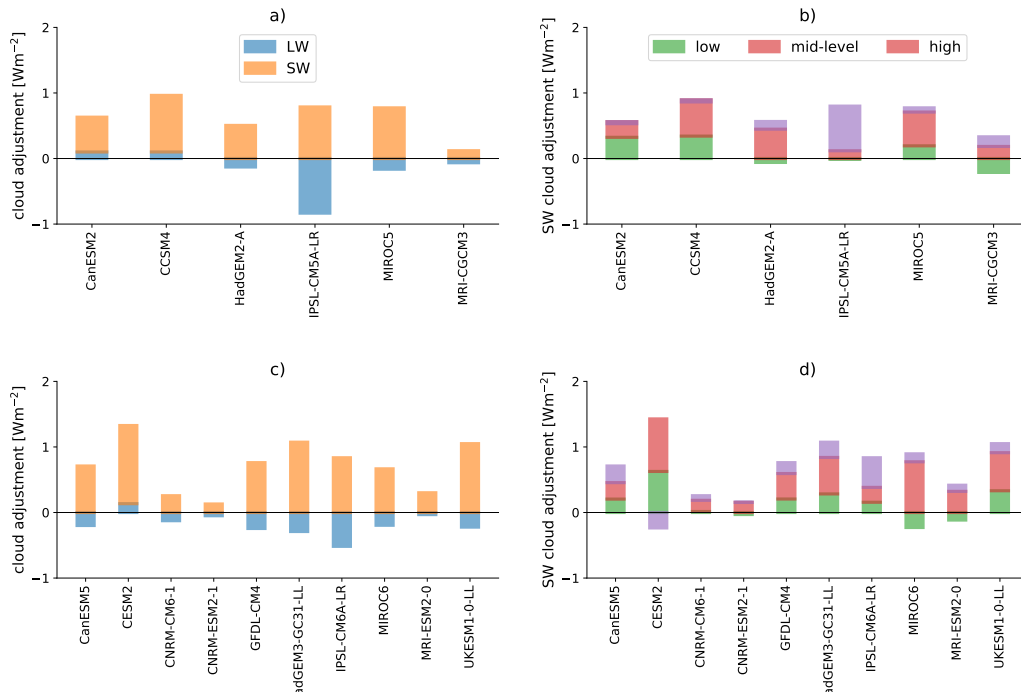
295 We have investigated this possibility in two ways. First, we calculated the cloud ad-  
 296 justments in aquaplanet simulations with seven CMIP6 models which outputted ISCCP  
 297 data. These cloud adjustments are independent of land models, and can be compared with  
 298 the results of *Ringer et al.* [2014], who found an anti-correlation between the CRE adjust-  
 299 ments and the CRE responses in aquaplanet simulations with a subset of CMIP5 mod-  
 300 els. In CMIP6, the cloud adjustments are positively correlated with  $\lambda_{SW,CL}$  in the aqua-  
 301 planet simulations ( $r = 0.59$ , Figure 7a), and these adjustments are also well correlated  
 302 with the cloud adjustments in the Earth-like simulations ( $r = 0.81$ , Figure 7b). *Qin et al.*  
 303 [2022] found a similar change in the sign of the relationship between the CRE responses  
 304 to CO<sub>2</sub> forcing and the CRE feedbacks in the CMIP5 and CMIP6 aquaplanet simulations  
 305 (see their Table 1).

306 Second, we decomposed the total cloud adjustments in the comprehensive model  
 307 simulations into contributions over land regions and over ocean regions (Figure 7c). There  
 308 are no systematic differences in the magnitudes of the cloud adjustments over land be-  
 309 tween the generations, though comparing the cloud adjustments in the six modeling cen-  
 310 ters which provided fixed-SST simulations in both CMIP5 and CMIP6 shows that the ad-  
 311 justment over ocean is always larger in CMIP6 than in the corresponding CMIP5 model.  
 312 The CMIP6 models cluster more closely to the 1:1 line than the CMIP5 models.

313 Together, these two lines of evidence strongly suggest that changes in land models  
 314 are not responsible for the differences in cloud adjustments between the model genera-  
 315 tions, which are instead likely driven by changes in atmospheric physics.

## 320 **6.2 Contributions of different cloud types**

321 To better understand the nature of the cloud adjustments, we decomposed the net  
 322 adjustments into the longwave and shortwave components (LW and SW, respectively; left  
 323 panels of Figure 8). The SW component is substantially larger than the LW component in  
 324 all of the models, with the exception of IPSL-CM5A-LR, suggesting that low and/or mid-  
 325 level clouds are primarily driving the adjustments. This is confirmed in the right panels of  
 326 Figure 8, in which the adjustments are decomposed into contributions from low clouds  
 327 (bottom two levels of the *Zelinka et al.* [2013] cloud kernels, 900-740hPa mid-points),



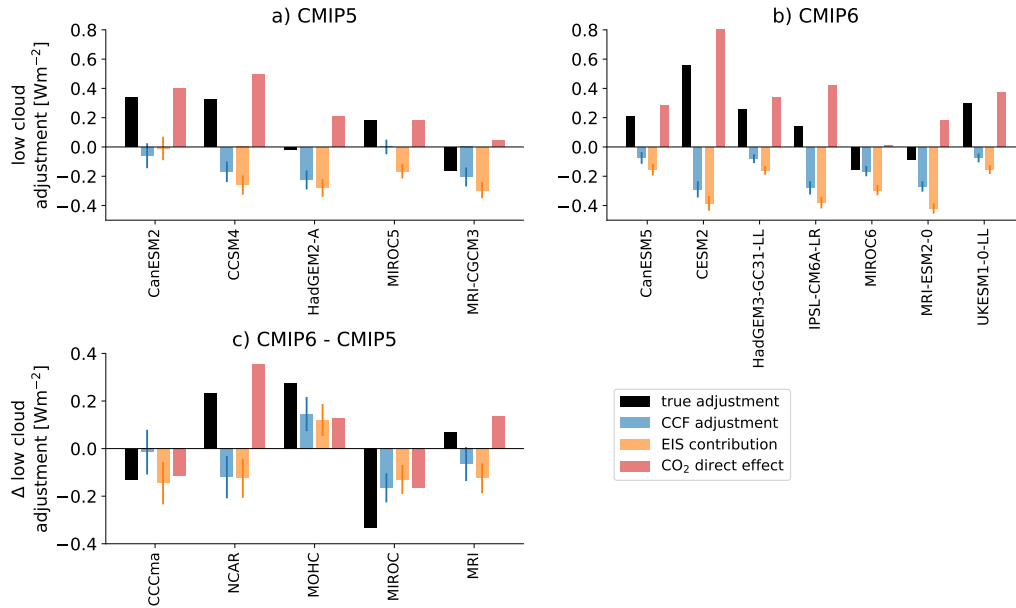
316 **Figure 8.** a) Decomposition of the total cloud adjustment into longwave (LW, blue),  
 317 orange) in the CMIP5 models. b) Decomposition of the SW cloud adjustment into contributions from low  
 318 (green), mid-level (red) and high (purple) clouds in the CMIP5 models. c) Same as panel a) but for the  
 319 CMIP6 models. d) Same as panel b) but for the CMIP6 models.

328 mid-level clouds (levels 3 and 4 of the cloud kernels, 620-500hPa mid-points) and high  
329 clouds (375hPa mid-point and above). Mid-level clouds are responsible for most of the  
330 intermodel differences in cloud adjustments, with smaller contributions from low clouds.  
331 The high cloud contribution is generally weak, except for in the IPSL models, particularly  
332 IPSL-CM5A-LR. We have not investigated why high clouds are so important for the ad-  
333 justment in these models.

334 While it is difficult to further determine what causes intermodel variations in mid-  
335 level cloud adjustments, we are able to provide some insight into the low cloud adjust-  
336 ments. This is helpful because the three CMIP6 models with the highest ECS values in-  
337 cluded here – CESM2, HadGEM3-GCM31-LL and the UKESM1-0-LL – have the three  
338 largest low cloud adjustments. Cloud Controlling Factors (CCFs) can be used to investi-  
339 gate how changes in governing meteorological conditions contribute to the large low cloud  
340 adjustments in these models (*Klein et al.* [2018], see Supplemental Material for more de-  
341 tails), and the residual between the true cloud adjustments and the CCF-derived adjust-  
342 ments can be taken as an estimate of CO<sub>2</sub>'s direct effect on low clouds. [As part of this  
343 analysis we have calculated the low cloud adjustments following *Scott et al.* [2020], which  
344 slightly modifies the *Zelinka et al.* [2013] method to remove the effects of mid- and high-  
345 level cloud masking. These estimates of the adjustments are qualitatively similar to the  
346 Zelinka et al.-derived estimates, but provide a more accurate estimate of the CO<sub>2</sub> direct  
347 effect.]

355 Figure 9 compares the true cloud adjustments in all of the available models, the  
356 CCF-derived low cloud adjustment estimates, and our estimates of the CO<sub>2</sub> direct effects.  
357 Also shown are the contributions of changes in Estimated Inversion Strength (EIS) to the  
358 CCF cloud adjustment. The complete CCF breakdown is shown in Supplemental Figure  
359 S2.

360 In all of the models, the CCF analysis suggests the low cloud adjustment will be  
361 negative (blue bars in panels a and b of Figure 9), and that this is largely driven by EIS  
362 changes – since surface temperatures are fixed, radiative heating in the free troposphere  
363 increases EIS, which in turn increases low cloud cover. Large CO<sub>2</sub> direct effect contribu-  
364 tions counter the EIS component, leading to the generally positive low cloud adjustments  
365 (red bars in panels a and b of Figure 9). The inferred low cloud reduction as a direct ef-  
366 fect of increasing CO<sub>2</sub> is consistent with theory and large eddy simulations, establishing



348 **Figure 9.** a) Results of cloud controlling factor analysis for available CMIP5 data. Black bars show the  
 349 “true” low cloud adjustments, calculated following *Scott et al.* [2020], blue bars show the CCF-derived cloud  
 350 adjustments, orange bars show the EIS contribution to the CCF-derived cloud adjustments and red bars show  
 351 the estimates CO<sub>2</sub> direct effect (difference between black and blue bars). b) Same as a) but for the avail-  
 352 able CMIP6 data. c) Differences between CMIP6 and CMIP5 models from the same modeling centers. The  
 353 method for estimating the errorbars is described in the Appendix, and the error bars in panel c are calculated  
 354 by adding the individual errors of two given models in quadrature.

367 confidence in our method for diagnosing its contribution to the overall low cloud adjust-  
368 ment [Bretherton, 2015; Tan et al., 2017; Sherwood et al., 2020]. Increasing CO<sub>2</sub> reduces  
369 cloud-top radiative cooling and hence the turbulent mixing within the boundary layer, re-  
370 sulting in reduced stratiform cloudiness.

371 Comparing the results for the five modeling center which provided the required  
372 data for both the CMIP5 and CMIP6 models (CCF kernels are not available for the IPSL-  
373 CM5A-LR model) shows large variations in the intergenerational differences (Figure 9c).  
374 For example, the two models with the largest increases in low cloud adjustment, CESM2  
375 and HadGEM, achieve this in different ways. In CESM2 the sensitivity to EIS actually in-  
376 creases – implying a more negative cloud adjustment – but this is countered by a much  
377 stronger CO<sub>2</sub> direct effect. In HadGEM3 the sensitivity to EIS decreases and the sensi-  
378 tivity to CO<sub>2</sub>'s direct effect increases, both contributing approximately equally to the total  
379 increase in the cloud adjustment.

## 380 **7 Summary and Discussion**

381 In this study, we have investigated the causes of the larger range of ECS values in  
382 CMIP6 compared to CMIP5. This required clarifying the definition of the radiative forc-  
383 ing: estimates of the forcing obtained by performing Gregory regressions for years 1-140  
384 of abrupt-4XCO<sub>2</sub> simulations are influenced by models' long-term feedbacks and tend to  
385 exhibit an apparent anti-correlation between the forcing and the SW cloud feedback. In-  
386 stead, using more accurate estimates of the forcing derived from fixed-SST simulations,  
387 we found that the cloud adjustment to the forcing and the SW cloud feedback are anti-  
388 correlated in CMIP5, while in CMIP6 the relationship is weakly positive. In turn, the SW  
389 cloud feedback and the forcing are negatively correlated in CMIP5 and weakly positively  
390 correlated in CMIP6 (the cloud adjustment is anti-correlated with the IRF in CMIP6,  
391 weakening the relationship between the forcing and the SW cloud feedback). The anti-  
392 correlation in CMIP5 damps the high end of ECS, as a model with a strong positive cloud  
393 feedback will have a smaller cloud adjustment and reduced forcing, whereas the CMIP6  
394 models with strong cloud feedbacks and large cloud adjustments have high ECS values  
395 over 5K.

396 We have been unable to identify a single factor responsible for the change between  
397 the two model generations, though our analysis was limited by the small number of fixed

398 SST simulations available for probing cloud adjustments. By calculating the cloud adjust-  
399 ments for aquaplanet simulations with CMIP6 models, we have shown that differences in  
400 atmospheric physics, and not in the the representation of land processes, are likely respon-  
401 sible for the opposite behavior in the two model generations. Furthermore, the differences  
402 in cloud adjustments across models are primarily driven by low and, especially, mid-level  
403 clouds, with the exception of the IPSL models for which high clouds make a larger con-  
404 tribution. We have used a Cloud Controlling Factor analysis to investigate the low cloud  
405 adjustments, and found that a negative EIS and a positive contribution from the CO<sub>2</sub> di-  
406 rect effect are the largest two components of the overall low cloud adjustment. However,  
407 these two factors vary substantially across models and there are no clear trends between  
408 the model generations.

409 Many of the trends identified here are driven by a small number of models: CESM2,  
410 HadGEM3-GCM31-LL and UKESM1-0-LL all have large, positive SW cloud feedbacks  
411 and cloud adjustments. Most of the other CMIP6 models with ECS values above 5K were  
412 originally derived from either the NCAR or MOHC models (e.g., E3SM and CIesm), as  
413 is UKESM1-0-LL. *Knutti et al.* [2013] has shown that models derived from the same origi-  
414 nal model can retain similarities for several generations, thus it may be that all the mod-  
415 els originally derived from those two modeling centers experienced a change in the sign  
416 of the relationship between cloud adjustments and cloud feedbacks between CMIP5 and  
417 CMIP6, which expanded the range of ECS between the model generations. An important  
418 exception, which merits further study, is the CanESM5 model, which has an ECS above  
419 5K, a moderate cloud adjustment, a relatively large total forcing and a relatively small net  
420 feedback that is largely driven by the LW cloud feedback, not the SW cloud feedback. In  
421 general, we believe that the results presented above argue for more simulations designed to  
422 probe the mechanisms of cloud adjustments and hence improve our understanding of what  
423 caused the greater range of ECS values in the CMIP6 generation of models.

## 424 **Acknowledgments**

425 We thank Chris Smith for sharing the CMIP6 cloud adjustment data and Masahiro Watan-  
426 abe and Miki Arai for sharing the MIROC6 fixed SST data. We also thank Tim Andrews  
427 for the suggestion to calculate the cloud adjustments for the aquaplanet simulations and  
428 Nadir Jeevanjee for helpful discussions. N.J.L. and C.J.W. were supported by the NOAA

429 Climate Program Office’s Modeling, Analysis, Predictions, and Projections program through  
 430 grant NA20OAR4310387.

### 431 **Open Research**

432 All CMIP data are available from the ESGF at *LLNL* [2022]. The cloud kernels  
 433 used to calculate the adjustments are available at *Zelinka* [2022] and the meteorological  
 434 cloud radiative kernels used in the CCF analysis are available at *Myers* [2022]. All analy-  
 435 sis and processing scripts will be made publicly available upon acceptance of the paper.

### 436 **References**

- 437 Andrews, T., J. M. Gregory, M. J. Webb, and K. E. Taylor (2012), Forcing, feedbacks and  
 438 climate sensitivity in cmip5 coupled atmosphere-ocean climate models, *Geophysical*  
 439 *Research Letters*, *39*(9), 109712.
- 440 Andrews, T., J. M. Gregory, and M. J. Webb (2015), The dependence of radiative forcing  
 441 and feedback on evolving patterns of surface temperature change in climate models.,  
 442 *Journal of Climate*, *28*(2), 1630–1648.
- 443 Andrews, T., M. B. Andrews, A. Bodas-Salcedo, G. S. Jones, T. Kuhlbrodt, J. Man-  
 444 ners, M. B. Menary, J. Ridley, M. A. Ringer, A. A. Sellar, C. A. Senior, and  
 445 Y. Tang (2019), Forcings, feedbacks, and climate sensitivity in hadgem3-gc3.1 and  
 446 ukesm1, *Journal of Advances in Modeling Earth Systems*, *11*(12), 4377–4394, doi:  
 447 <https://doi.org/10.1029/2019MS001866>.
- 448 Armour, K. C., C. M. Bitz, and G. H. Roe (2013), Time-Varying Climate Sensitivity from  
 449 Regional Feedbacks, *Journal of Climate*, *26*(13), 4518–4534, doi:10.1175/JCLI-D-12-  
 450 00544.1.
- 451 Bretherton, C. S. (2015), Insights into low-latitude cloud feedbacks from high-resolution  
 452 models, *Philosophical Transactions of the Royal Society A: Mathematical, Physical and*  
 453 *Engineering Sciences*, *373*(2054), 20140,415.
- 454 Caldwell, P. M., M. D. Zelinka, K. E. Taylor, and K. Marvel (2016), Quantifying the  
 455 Sources of Intermodel Spread in Equilibrium Climate Sensitivity, *Journal of Climate*,  
 456 *29*(2), 513–524, doi:10.1175/JCLI-D-15-0352.1, publisher: American Meteorological  
 457 Society Section: Journal of Climate.
- 458 Chung, E.-S., and B. J. Soden (2015), An Assessment of Direct Radiative Forcing, Ra-  
 459 diative Adjustments, and Radiative Feedbacks in Coupled Ocean–Atmosphere Mod-

- 460 els, *Journal of Climate*, 28(10), 4152–4170, doi:10.1175/JCLI-D-14-00436.1, publisher:  
461 American Meteorological Society Section: Journal of Climate.
- 462 Dong, Y., K. C. Armour, M. D. Zelinka, C. Proistosescu, D. S. Battisti, C. Zhou, and  
463 T. Andrews (2020), Intermodel Spread in the Pattern Effect and Its Contribution to Cli-  
464 mate Sensitivity in CMIP5 and CMIP6 Models, *Journal of Climate*, 33(18), 7755–7775,  
465 doi:10.1175/JCLI-D-19-1011.1, publisher: American Meteorological Society Section:  
466 Journal of Climate.
- 467 Forster, P., T. Storelvmo, K. Armour, W. Collins, J.-L. Dufresne, D. Frame, D. J. Lunt,  
468 T. Mauritsen, M. D. Palmer, M. Watanabe, M. Wild, and H. Zhang (2021), The earth-  
469 's energy budget, climate feedbacks, and climate sensitivity, in *Climate Change*  
470 *2021: The Physical Science Basis. Contribution of Working Group I to the Sixth Assess-*  
471 *ment Report of the Intergovernmental Panel on Climate Change*, edited by V. Masson-  
472 Delmotte, P. Zhai, A. Pirani, S. L. Connors, C. Péan, S. Berger, N. Caud, Y. Chen,  
473 L. Goldfarb, M. I. Gomis, M. Huang, K. Leitzell, E. Lonnoy, J. B. R. Matthews, T. K.  
474 Maycock, T. Waterfield, O. Yelekci, R. Yu, and B. Zhou, Cambridge University Press,  
475 Geneva, Switzerland.
- 476 Forster, P. M. (2016), Inference of climate sensitivity from analysis of earth's energy  
477 budget, *Annual Reviews of Earth and Planetary Sciences*, 44(0), 85–106.
- 478 Forster, P. M., T. Andrews, P. Good, J. M. Gregory, L. S. Jackson, and M. Zelinka (2013),  
479 Evaluating adjusted forcing and model spread for historical and future scenarios in the  
480 cmip5 generation of climate models, *Journal of Geophysical Research: Atmospheres*,  
481 118, 1139–1150.
- 482 Forster, P. M., T. Richardson, A. C. Maycock, C. J. Smith, B. H. Samset, G. Myhre,  
483 T. Andrews, R. Pincus, and M. Schulz (2016), Recommendations for diagnosing ef-  
484 fective radiative forcing from climate models for CMIP6, *Journal of Geophysical Re-*  
485 *search: Atmospheres*, 121(20), 12,460–12,475, doi:10.1002/2016JD025320, \_eprint:  
486 <https://onlinelibrary.wiley.com/doi/pdf/10.1002/2016JD025320>.
- 487 Geoffroy, O., D. Saint-Martin, G. Bellon, A. Voltaire, D. J. L. Olivie, and S. Tyteca  
488 (2013), Transient climate response in a two-layer energy-balance model. part ii: Rep-  
489 resentation of the efficacy of deep-ocean heat uptake and validation for cmip5 aogcms,  
490 *Journal of Climate*, 26(6), 1859–1876.
- 491 Gregory, J., and M. Webb (2008), Tropospheric adjustment induces a cloud component in  
492 CO<sub>2</sub> forcing, *Journal of Climate*, 21(1), 58–71.

- 493 Gregory, J. M., W. J. Ingram, M. A. Palmer, G. S. Jones, P. A. Stott, R. B. Thorpe, J. A.  
 494 Lowe, T. C. Johns, and K. D. Williams (2004), A new method for diagnosing radiative  
 495 forcing and climate sensitivity, *Geophysical Research Letters*, *31*, L03,205.
- 496 Hansen, J., M. Sato, R. Ruedy, L. Nazarenko, A. Lacis, G. A. Schmidt, G. Russell,  
 497 I. Aleinov, M. Bauer, S. Bauer, N. Bell, B. Cairns, V. Canuto, M. Chandler, Y. Cheng,  
 498 A. Del Genio, G. Faluvegi, E. Fleming, A. Friend, T. Hall, C. Jackman, M. Kelley,  
 499 N. Y. Kiang, D. Koch, J. Lean, J. Lerner, K. Lo, S. Menon, R. L. Miller, P. Minnis,  
 500 T. Novakov, V. Oinas, J. P. Perlwitz, J. Perlwitz, D. Rind, A. Romanou, D. Shindell,  
 501 P. Stone, S. Sun, N. Tausnev, D. Thresher, B. Wielicki, T. Wong, M. Yao, and S. Zhang  
 502 (2005), Efficacy of climate forcings, *J. Geophys. Res.*, *110*, D18,104.
- 503 Kamae, Y., and M. Watanabe (2012), On the robustness of tropospheric adjustment in  
 504 CMIP5 models, *Geophysical Research Letters*, *39*(23), doi:10.1029/2012GL054275,  
 505 \_eprint: <https://onlinelibrary.wiley.com/doi/pdf/10.1029/2012GL054275>.
- 506 Klein, S. A., and C. Jakob (1999), Validation and sensitivities of frontal clouds simulated  
 507 by the ecmwf model, *Monthly Weather Review*, *127*(2), 2514–2531.
- Klein, S. A., A. Hall, J. R. Norris, and R. Pincus (2018), Low-Cloud Feedbacks from  
 Cloud-Controlling Factors: A Review, in *Shallow Clouds, Water Vapor, Circulation, and  
 Climate Sensitivity*, edited by R. Pincus, D. Winker, S. Bony, and B. Stevens, pp. 135–  
 157, Springer International Publishing, Cham, doi:10.1007/978-3-319-77273-8\_7.
- 508 Knutti, R., D. Masson, and A. Gettelman (2013), Climate model genealogy: Generation  
 509 cmip5 and how we got there, *Geophysical Research Letters*, *40*(6), 1194–1199, doi:  
 510 <https://doi.org/10.1002/grl.50256>.
- 511 LLNL (2022), Earth system grid federation – cmip data, <https://esgf->  
 512 [node.llnl.gov/projects/esgf-llnl/](https://node.llnl.gov/projects/esgf-llnl/), [Dataset].
- 513 Lutsko, N. J., M. Popp, R. H. Nazarian, and A. L. Albright (2021), Emergent constraints on  
 514 regional cloud feedbacks, *Geophysical Research Letters*, *48*(10), e2021GL092,934, doi:  
 515 <https://doi.org/10.1029/2021GL092934>, e2021GL092934 2021GL092934.
- 516 Myers, T. A. (2022), Meteorological cloud radiative kernels,  
 517 <https://sites.google.com/site/myerstimothy/meteorological-cloud-radiative-kernels>,  
 518 [Computational product].
- 519 Myers, T. A., R. C. Scott, M. D. Zelinka, S. A. Klein, J. R. Norris, and P. M. Caldwell  
 520 (2021), Observational constraints on low cloud feedback reduce uncertainty of climate  
 521 sensitivity, *Nature Climate Change*, *11*(6), 501–507, doi:10.1038/s41558-021-01039-0.

- 522 Qin, Y., M. D. Zelinka, and S. A. Klein (2022), On the correspondence between  
523 atmosphere-only and coupled simulations for radiative feedbacks and forcing from  
524 *co2*, *Journal of Geophysical Research: Atmospheres*, *127*(3), e2021JD035460, doi:  
525 <https://doi.org/10.1029/2021JD035460>, e2021JD035460 2021JD035460.
- 526 Ringer, M. A., T. Andrews, and M. J. Webb (2014), Global-mean radiative feed-  
527 backs and forcing in atmosphere-only and coupled atmosphere-ocean climate  
528 change experiments, *Geophysical Research Letters*, *41*(11), 4035–4042, doi:  
529 <https://doi.org/10.1002/2014GL060347>.
- 530 Scott, R. C., T. A. Myers, J. R. Norris, M. D. Zelinka, S. A. Klein, M. Sun, and D. R.  
531 Doelling (2020), Observed Sensitivity of Low-Cloud Radiative Effects to Meteorologi-  
532 cal Perturbations over the Global Oceans, *Journal of Climate*, *33*(18), 7717–7734, doi:  
533 10.1175/JCLI-D-19-1028.1, publisher: American Meteorological Society Section: Journal  
534 of Climate.
- 535 Sherwood, S. C., S. Bony, O. Boucher, C. Bretherton, P. M. Forster, J. M. Gregory, and  
536 B. Stevens (2015), Adjustments in the forcing-feedback framework for understanding cli-  
537 mate change, *Bulletin of the American Meteorological Society*, *96*(6), 217–228.
- 538 Sherwood, S. C., M. J. Webb, J. D. Annan, K. C. Armour, P. M. Forster, J. C. Hargreaves,  
539 G. Hegerl, S. A. Klein, K. D. Marvel, E. J. Rohling, M. Watanabe, T. Andrews, P. Bracon-  
540 not, C. S. Bretherton, G. L. Foster, Z. Hausfather, A. S. v. d. Heydt, R. Knutti, T. Mau-  
541 ritsen, J. R. Norris, C. Proistosescu, M. Rugenstein, G. A. Schmidt, K. B. Tokarska, and  
542 M. D. Zelinka (2020), An assessment of Earth’s climate sensitivity using multiple lines of  
543 evidence, *Reviews of Geophysics*, *n/a*(*n/a*), e2019RG000,678.
- 544 Smith, C. J., R. J. Kramer, G. Myhre, K. Alterskjær, W. Collins, A. Sima, O. Boucher, J.-  
545 L. Dufresne, P. Nabat, M. Michou, S. Yukimoto, J. Cole, D. Paynter, H. Shiogama, F. M.  
546 O’Connor, E. Robertson, A. Wiltshire, T. Andrews, C. Hannay, R. Miller, L. Nazarenko,  
547 A. Kirkevåg, D. Olivić, S. Fiedler, R. Pincus, and P. M. Forster (2020), Effective radia-  
548 tive forcing and adjustments in CMIP6 models, *preprint*, Radiation/Atmospheric Mod-  
549 elling/Troposphere/Physics (physical properties and processes), doi:10.5194/acp-2019-  
550 1212.
- 551 Soden, B. J., A. J. Broccoli, and R. S. Hemler (2004), On the Use of Cloud Forcing to  
552 Estimate Cloud Feedback, *Journal of Climate*, *17*(19), 3661–3665, doi:10.1175/1520-  
553 0442(2004)017<3661:OTUOCF>2.0.CO;2, publisher: American Meteorological Society  
554 Section: Journal of Climate.

- 555 Soden, B. J., I. M. Held, R. Colman, K. M. Shell, J. T. Kiehl, and C. A. Shields (2008),  
556 Quantifying climate feedbacks using radiative kernels, *Journal of Climate*, *21*(6), 3504–  
557 3520.
- 558 Tan, Z., T. Schneider, J. Teixeira, and K. G. Pressel (2017), Large-eddy simulation of sub-  
559 tropical cloud-topped boundary layers: 2. Cloud response to climate change: LES OF  
560 LOW CLOUDS UNDER CLIMATE CHANGE, *Journal of Advances in Modeling Earth  
561 Systems*, *9*(1), 19–38, doi:10.1002/2016MS000804.
- 562 Vial, J., J.-L. Dufresne, and S. Bony (2013), On the interpretation of inter-model spread in  
563 cmip5 climate sensitivity estimates., *Climate Dynamics*, *41*(1), 3339–3362.
- 564 Webb, M., C. Senior, S. Bony, and J. J. Marcette (2001), Combining erbe and isccp data to  
565 assess clouds in the hadley centre, ecmwf and lmd atmospheric climate models, *Climate  
566 Dynamics*, *17*(2), 905–922.
- 567 Winton, M., K. Takahashi, and I. M. Held (2010), Importance of ocean heat uptake efficacy  
568 to transient climate change, *Journal of Climate*, *23*(6), 2333–2344.
- 569 Xie, S.-P. (2020), Ocean warming pattern effect on global and regional climate change,  
570 *AGU Advances*, *1*(1), e2019AV000,130, doi:https://doi.org/10.1029/2019AV000130,  
571 e2019AV000130 2019AV000130.
- 572 Zelinka, M. (2022), Cloud radiative kernels, [https://github.com/mzelinka/cloud-  
573 radiative-  
kernels/tree/master/data](https://github.com/mzelinka/cloud-radiative-kernels/tree/master/data), [Computational product].
- 574 Zelinka, M. D., S. A. Klein, and K. E. Taylor (2013), Contributions of different cloud types  
575 to feedbacks and rapid adjustments in cmip5, *Journal of Climate*, *26*, 5007–5027.
- 576 Zelinka, M. D., T. A. Myers, D. T. McCoy, S. PoáŕŔChedley, P. M. Caldwell, P. Ceppi,  
577 S. A. Klein, and K. E. Taylor (2020), Causes of Higher Climate Sensitivity in CMIP6  
578 Models, *Geophysical Research Letters*, *47*(1), e2019GL085,782.